Maker Fringes: A Detailed Comparison of Theory and Experiment for Isotropic and Uniaxial Crystals

J. Jerphagnon, and S. K. Kurtz

Citation: Journal of Applied Physics **41**, 1667 (1970); doi: 10.1063/1.1659090
View online: https://doi.org/10.1063/1.1659090
View Table of Contents: http://aip.scitation.org/toc/jap/41/4
Published by the American Institute of Physics

Maker Fringes: A Detailed Comparison of Theory and Experiment for Isotropic and Uniaxial Crystals

J. JERPHAGNON* AND S. K. KURTZ†
Bell Telephone Laboratories, Incorporated, Murray Hill, New Jersey 07974
(Received 28 May 1969; in final form 2 September 1969)

A complete theory of Maker fringes in nonabsorbing isotropic and uniaxial crystals has been derived which includes all the corrections necessary for making precise determinations of nonlinear optical coefficients. These corrections include finite beamwidth effects and multiple reflection corrections. Comparison of this theory with extensive experimental data on the Maker fringes in quartz, ADP, and KDP shows agreement to within the experimental accuracy of about 5% on the Maker fringe envelopes and to better than 1% on the coherence lengths. We conclude from this study that a careful analysis of Maker fringes can yield precise values of the nonlinear optical coefficients and coherence lengths in isotropic and uniaxial crystals. This is of great importance in establishing *accurate* and *reliable* standards in the field of nonlinear optics.

I. INTRODUCTION

It is obviously of great interest to measure with a high accuracy (within 5% or less) the nonlinear optical (NLO) coefficients of materials to be used as standards. So far, two different experimental techniques have been widely used to measure NLO coefficients. The first method is concerned with the possibility of obtaining phase matching between the fundamental and the harmonic waves. It has been studied in great detail[1] and has led to the absolute measurement of $d_{36}^{2\omega}$ in ADP[2,3] with a quoted accuracy of about 10%.

The second method of measuring NLO coefficients can be used for all materials, whether phase matchable or not; it is the technique used by Maker *et al.*[4] on quartz to demonstrate the interference between the bound and free harmonic waves. By varying the incidence angle of a laser beam on a plane parallel sample of NLO material, the intensity of the second harmonic generated and transmitted is found to oscillate in a periodic fashion. For highly absorbing materials, the transmitted second harmonic vanishes. Nevertheless, the NLO coefficients can be deduced from the measurement of the reflected second-harmonic wave at the boundary of the material.[5,6]

The coherence length between the bound and free harmonic waves can be deduced from the spacing between the minima (or maxima) of the Maker fringes while the NLO coefficient is correlated with the peak amplitudes of the oscillations. Several authors[7–11] have used the Maker fringe technique to measure NLO coefficients relative to a standard NLO coefficient such as $d_{36}^{2\omega}$ of KDP. There has, however, been a wide range of variation (several times quoted experimental errors) in these results. For example, the published values of the important ratio $d_{36}^{2\omega}(\text{ADP})/d_{36}^{2\omega}(\text{KDP})$ vary by 45%. This has caused one of the authors (S.K.K.) considerable difficulty in assembling a definitive table[12] of NLO coefficients.

The purpose of this work is to make a detailed theoretical analysis of the Maker fringes including a thorough investigation of all possible sources of experimental error and thereby demonstrate that the maker fringe method provides a powerful tool for making accurate relative measurements of NLO coefficients. In this article we present a detailed theory of the Maker fringes for both isotropic and uniaxial crystals and compare with the experimental results for each of three materials, quartz, ADP, and KDP, over a wide range of angles of incidence.

The precise measurement of the relative values for $d_{11}^{2\omega}$ of quartz, $d_{36}^{2\omega}$ of ADP and $d_{36}^{2\omega}$ of KDP will be published elsewhere.

II. THEORY

Assume a fundamental laser beam, of fixed power P_ω, linearly polarized electric field $\mathbf{E}_\omega$ and wave vector $\mathbf{k}_\omega$, which is incident on a nonlinear crystal in the form of a plane parallel slab of thickness L, rotating about an axis perpendicular to $\mathbf{k}_\omega$. Let θ be the incidence angle for the laser beam on the crystal measured between the beam direction and the surface normal as shown in Fig. 1.

Inside the crystal, the electric field E'_ω at angular frequency at ω induces a nonlinear polarization $\mathcal{P}_{2\omega}'$ which radiates electromagnetic waves of angular frequency 2ω. This wave is called the "bound" harmonic wave. There is in addition to the "bound" harmonic wave, a "free" harmonic wave (of angular frequency 2ω) generated at the input surface. These "bound" and "free" harmonic waves have in general different velocities, giving rise to interference fringes in the harmonic power $P_{2\omega}''$ as the slab is rotated. The harmonic power $P_{2\omega}''$ coming from the crystal is thus calculated as a function of θ by examining the interference between the bound and free wave harmonic solutions of Maxwell's equations.

The crystal is assumed to be without absorption losses at both the fundamental and harmonic frequencies. Part of the theory applicable to this situation has been given by Bloembergen and Pershan.[5] In the following we recapitulate this theory and extend it to include all the necessary refinements. Let us assume

TABLE I. The independent, nonvanishing (assuming Kleinman's relations) NLO coefficients for all uniaxial and cubic classes are listed along with the Miller indices of the sample faces, the direction of the electric field for both fundamental and harmonic waves, the axis of rotation, the indices of refraction involved and the projection factor $p(\theta)$, required for the separate determination of each NLO coefficient. In all cases the nonlinear polarization is parallel to the electric field at 2ω and is perpendicular to the plane of incidence.

NLO coeff	Class	Sample orientation	E_ω	$E_{2\omega}$	Rotation	n_ω	$n_{2\omega}$	$p(\theta)$
d_{11}	$3(C_3)$, $32(D_3)$ $\bar{6}(C_{3h})$, $\bar{6}m2(D_{3h})$	$(0hk)$	$\parallel x$	$\parallel x$	$\parallel x$	n_ω^0	$n_{2\omega}^0$	1
d_{22}	$3(C_3)$, $3m(C_{3v})$ $\bar{6}(C_{3h})$	$(h0k)$	$\parallel y$	$\parallel y$	$\parallel y$	n_ω^0	$n_{2\omega}^0$	1
d_{33}	$4(C_4)$, $4mm(C_{4v})$ $3(C_3)$, $3m(C_{3v})$ $6(C_6)$, $6mm(C_{6v})$	$(hk0)$	$\parallel z$	$\parallel z$	$\parallel z$	n_ω^e	$n_{2\omega}^e$	1
d_{31}	$4(C_4)$, $\bar{4}(S_4)$, $4mm(C_{4v})$ $3(C_3)$, $3m(C_{3v})$ $6(C_6)$, $6mm(C_{6v})$	$(hk0)$	$\perp z$	$\parallel z$	$\parallel z$	n_ω^0	$n_{2\omega}^e$	1
d_{36}	$\bar{4}(S_4)$, $\bar{4}2m(D_{2d})$ $23(T_d)$, $\bar{4}3m(T)$	(110)	$\perp z$	$\parallel z$	$\parallel z$	n_ω^0	$n_{2\omega}^e$	$2\cos(\theta_\omega'+\pi/4)$ $\times\cos(\theta_\omega'-\pi/4)$

that the Poynting vector is collinear with the wave vector $\mathbf{k}$ for both harmonic and fundamental waves. This occurs when the crystal is isotropic (cubic system) or uniaxial in the particular cases $\mathbf{E}_\omega'$ and $\mathbf{E}_{2\omega}'$ are either parallel or perpendicular to the optic axis. Our assumption does not lead to a loss of generality as far as the measurement of NLO coefficients in isotropic or uniaxial crystals is concerned: Assuming Kleinman's[13] relations, it is possible, for any allowed NLO coefficient of these crystals, to choose the crystallographic orientation of the sample in such a way that the Maker fringe experiment involves only this nonlinear coefficient, $\mathbf{E}_\omega'$ and $\mathbf{E}_{2\omega}'$ being either parallel or perpendicular to the optic axis as indicated in Table I. We will consider in another paper the general case of an anisotropic crystal.

We first calculate $P_{2\omega}''$ assuming the transverse dimension of the sample is infinite and there are no effects due to the size of the laser beam. In other words, we use the plane wave approximation.

The calculation can be carried out in three steps by examining (A) the boundary conditions at the input face of the sample, (B) the generation and propagation of the free and bound harmonic waves, (C) the boundary conditions at the output face of the crystal.

A. Boundary Conditions at the Input Face of the Sample

1. Fundamental Wave

Using Snell's law and Fresnel's formulas we get for the refraction angle θ_ω'

$$\sin\theta_\omega' = \sin\theta/n_\omega \tag{1}$$

(all the refractive indices are with respect to air) and for the wave vector $\mathbf{k}_\omega'$

$$|\,\mathbf{k}_\omega'\,| = n_\omega(\omega/c). \tag{2}$$

The amplitude of the electric field $\mathbf{E}_\omega'$ is

$$|\,\mathbf{E}_\omega'\,| = t_\omega'\,|\,\mathbf{E}_\omega\,|, \tag{3}$$

where

$$t_\omega' = 2\cos\theta/(n_\omega\cos\theta_\omega' + \cos\theta) \tag{4}$$

if $\mathbf{E}_\omega$ is perpendicular to the plane of incidence, or

$$t_\omega' = 2\cos\theta/(n_\omega\cos\theta + \cos\theta_\omega') \tag{5}$$

if $\mathbf{E}_\omega$ is parallel to the plane of incidence.

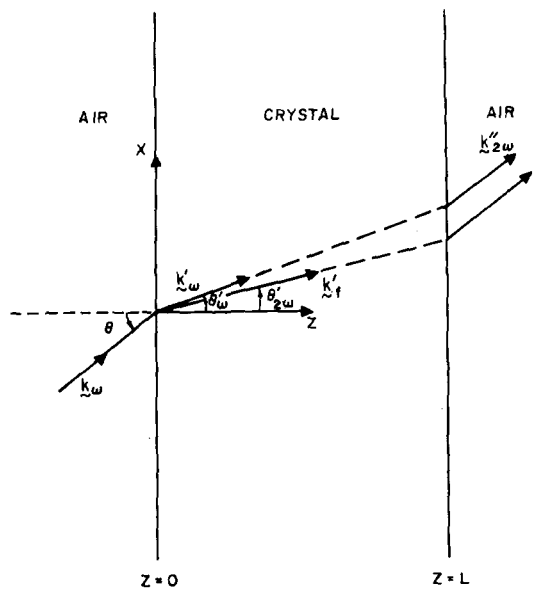

FIG. 1. Propagation of the fundamental and second-harmonic waves. The Y axis is perpendicular to the plane of the figure.

2. Bound and Free Harmonic Waves

Because of the presence of a nonlinear polarization in the crystal, there is, as we show in Appendix A, a reflected wave in air at 2ω and two harmonic waves in the crystal with the following wave vectors.

For the free wave:

$$\sin\theta_{2\omega}' = \sin\theta/n_{2\omega}, \tag{6}$$

$$|\,\mathbf{k}_f\,| = n_{2\omega}(2\omega/c). \tag{7}$$

For the bound wave:

$$\sin\theta_{\omega}' = \sin\theta/n_{\omega}, \tag{8}$$

$$|\,\mathbf{k}_b\,| = n_{\omega}(2\omega/c). \tag{9}$$

B. Generation and Propagation of the Harmonic Waves

The nonlinear polarization $\mathcal{P}_{2\omega}'$ has to be introduced in Maxwell's equations to determine the electric field $\mathbf{E}_{2\omega}'$ at each point of the crystal. As shown by the detailed calculations given in Appendix A, the general expression for $\mathbf{E}_{2\omega}'$ is

$$\mathbf{E}_{2\omega}' = \hat{e}_f E_f' \exp(i\mathbf{k}_f\cdot\mathbf{r}) + \hat{e}_b[4\pi\mathcal{P}_{2\omega}'/(n_{\omega}^2 - n_{2\omega}^2)] \times\exp(i\mathbf{k}_b\cdot\mathbf{r}). \tag{10}$$

The first term represents the free wave and the second term the bound wave. $\hat{e}_b$ is a function of $\hat{p}$, the unit vector along $\mathcal{P}_{2\omega}'$, $\mathbf{k}_b$, and $\mathbf{k}_f$ given in Eq. (A7). The boundary conditions for electric and magnetic fields at $Z=0$ determine E_f' as a function of $\mathcal{P}_{2\omega}'$, and $\hat{e}_f$. [See Eqs. (A26) and (A32).]

C. Boundary Conditions at the Output Face of the Crystal

Both fundamental and harmonic waves are reflected at the back surface of the slab. Strictly speaking, it is necessary to consider multiple reflections at the output face and at the input face of the crystal and also the nonlinear interactions between all the waves generated in this manner. If the refractive index of the crystal is very high, these interactions may be important. An evaluation of these phenomena is described in Appendix B, where we show that in the case of crystals with low indices of refraction the correction $\mathcal{R}$ is close to 1 and quite independent of θ. It can therefore be omitted for materials of low index. At the output face of the crystal there is in air only a free harmonic wave with the wave vector

$$\mathbf{k}_{2\omega}'' = 2\mathbf{k}_{\omega}.$$

Applying then the boundary conditions on the electric and magnetic fields at the output face of the crystal, we calculate the amplitude of the transmitted electric field $E_{2\omega}''$ (see Appendix A). Insofar as the multiple reflections are neglected, the derivations are made without the customary[5] assumption

$$E_f' \cong 4\pi\mathcal{P}_{2\omega}'(n_{\omega}^2 - n_{2\omega}^2)^{-1}$$

at the output face of the crystal.

The intensity $I_{2\omega}''$ of the transmitted second-harmonic beam is deduced from

$$I_{2\omega}'' = (c/8\pi)\,\mathbf{E}_{2\omega}'' \times \mathbf{H}_{2\omega}''^{*} = (c/8\pi)\,|\,E_{2\omega}''\,|^2.$$

Hence, the second-harmonic power can be easily calculated. We define a transmission factor $T_{2\omega}''$ as follows:

$$T_{2\omega}'' = 2n_{2\omega}\cos\theta_{2\omega}' \times \frac{(\cos\theta + n_{\omega}\cos\theta_{\omega}')(n_{\omega}\cos\theta_{\omega}' + n_{2\omega}\cos\theta_{2\omega}')}{(n_{2\omega}\cos\theta_{2\omega}' + \cos\theta)^3} \tag{11}$$

if the nonlinear polarization $\mathcal{P}_{2\omega}'$ is perpendicular to the plane of incidence, and

$$T_{2\omega}'' = 2n_{2\omega}\cos\theta_{2\omega}' \times \frac{(n_{\omega}\cos\theta + \cos\theta_{\omega}')(n_{2\omega}\cos\theta_{\omega}' + n_{\omega}\cos\theta_{2\omega}')}{(n_{2\omega}\cos\theta_{2\omega}' + \cos\theta)^3} \tag{12}$$

if the nonlinear polarization is in the plane of incidence. We take

$$\Psi = (\pi L/2)\,(4/\lambda)\,(n_{\omega}\cos\theta_{\omega}' - n_{2\omega}\cos\theta_{2\omega}'). \tag{13}$$

$I_{2\omega}''$ can be written as the sum of two terms: one is dependent on Ψ and the other is not [see Eqs. (A36) and (A39)]. The second term has an amplitude several orders-of-magnitude smaller than the maximum of the first one; hence we can drop it in the final step. With these definitions and results the transmitted second-harmonic power can be written

$$P_{2\omega}'' = (512\pi^3/A)\,d^2 t_{\omega}'^4 T_{2\omega}''\mathcal{R}(\theta)\,p^2(\theta) \times P_{\omega}^2[1/(n_{\omega}^2 - n_{2\omega}^2)^2]\sin^2\Psi, \tag{14}$$

where P_{ω} is the fundamental power, c is the light velocity in air, A is the beam area, d is the NLO coefficient, t_{ω}' and $T_{2\omega}''$ are the transmission factors, as defined by Eqs. (4), (5), (11), (12), $\mathcal{R}(\theta)$ is the multiple reflection correction (Appendix B), L is the sample thickness, λ is the wavelength of the fundamental beam in air, $p(\theta)$ is a projection factor which depends on the form of the nonlinear tensor $\mathbf{d}$ and on the direction of $\mathcal{P}_{2\omega}'$ compared with the plane of incidence. The general formula for $p(\theta)$ is given in Appendix A.

The relation (14) has been obtained assuming the electric field of the incident laser beam is of constant amplitude over the entire beam area A, which is in turn large compared to L^2. Hence, we were allowed to neglect the fact that inside the crystal the bound and free harmonic waves are not traveling in exactly the same direction.

If A is not large compared to L^2, an additional so-called "beam size" correction has to be considered.

We show in Appendix C how this correction can be calculated in the case of a Gaussian laser beam. The

result is

$$P_{2\omega}'' = (512\pi^2/cw^2)\, d^2 t_\omega'^4 T_{2\omega}'' \mathcal{R}(\theta)\, p_{(\theta)}^2 \times P_\omega^2 [1/(n_\omega^2 - n_{2\omega}^2)^2] \mathcal{B}(\theta) \sin^2\Psi, \quad (15)$$

$$\mathcal{B}(\theta) = \exp[-(L^2/w^2)\cos^2\theta(\tan\theta_\omega' - \tan\theta_{2\omega}')^2]. \quad (16)$$

w is the spot radius of the Gaussian beam.[14]

There is a significant difference between Eqs. (14) and (15) only in the case of thick and very dispersive materials or if a tightly focused laser beam is used. The difference is equal to zero for normal incidence; so we can see that it is important only for large values of θ.

D. Angular Dependence and Envelope Function

1. General Formulation

Let us now consider the variation of the transmitted second-harmonic power $P_{2\omega}''$ as a function of θ. As given in Eqs. (14) and (15), $P_{2\omega}''$ is an oscillating function of θ with minima equal to zero. Examination of Eqs. (14) and (15) shows that the positions of the minima are exactly determined by the zeros of

$$\sin^2\Psi = \sin^2[(\pi L/2)(4/\lambda)(n_\omega \cos\theta_\omega' - n_{2\omega}\cos\theta_{2\omega}')]$$

and therefore depend only on the thickness of the sample and the dispersion of the refractive index. By contrast the positions of the maxima can be slightly shifted by additional terms (e.g., transmission factor $t_\omega'^4$).

The phase difference between the bound and free harmonic waves is equal to 2Ψ. Because the surfaces of constant phase mismatch in the crystal are the planes perpendicular to $\hat{Z}$, we define, for each value of θ, a coherence length

$$l_c(\theta) = \pi/(\mathbf{k}_b - \mathbf{k}_f)\cdot\hat{Z} = \lambda/4\,|\, n_\omega\cos\theta_\omega' - n_{2\omega}\cos\theta_{2\omega}'\,| \quad (17)$$

and the oscillating factor becomes

$$\sin^2[\pi L/2l_c(\theta)].$$

At normal incidence the coherence length is

$$l_c = \lambda/4\,|\, n_\omega - n_{2\omega}\,|. \quad (18)$$

The relative amplitudes of the maxima depend on

$$t_\omega'^4 T_{2\omega}'' \mathcal{R}(\theta)\, p^2(\theta)\, \mathcal{B}(\theta)$$

and the equation for the envelope of the Maker fringes is

$$P_M(\theta) = (512\pi^2/cw^2)\, d^2 t_\omega'^4 T_{2\omega}'' p^2(\theta)\mathcal{R}(\theta)\mathcal{B}(\theta) \times [P_\omega^2/(n_\omega^2 - n_{2\omega}^2)^2]. \quad (19)$$

For normal incidence we get

$$P_M(0) = (512\pi^2/cw^2)\, d^2 [16/(n_\omega+1)^3(n_{2\omega}+1)^3] \times p^2(0)\mathcal{R}(0)[2n_{2\omega}/(n_\omega+n_{2\omega})][1/(n_\omega - n_{2\omega})^2] P_\omega^2. \quad (20)$$

Knowing the values of the refractive index at ω and 2ω, it is possible to compute the theoretical shape of the Maker fringes as a function of angle for a given thickness L of a given material using a computer program for Eq. (15).

2. Application to Several Specific Cases

a. Quartz. Point Group 32—z is the threefold axis, x a twofold axis. The induced nonlinear polarization has components,

$$\mathcal{P}_x = d_{11}E_x^2 - d_{11}E_y^2 + 2d_{14}E_zE_y,$$
$$\mathcal{P}_y = -2d_{14}E_zE_x - 2d_{11}E_xE_y,$$
$$\mathcal{P}_z = 0.$$

According to Kleinman relations[13] $d_{14}=0$. We distinguish two cases,

(1) The input and output faces of the sample are (011) and rotation is about the x axis. The laser beam is polarized along x. The fundamental wave is ordinary and perpendicular to the incidence plane with transmission coefficient,

$$t_\omega'(\theta) = 2\cos\theta/(n_\omega^0\cos\theta_\omega' + \cos\theta).$$

The nonlinear polarization is parallel to x and perpendicular to the incidence plane. Hence the projection factor $p(\theta)$ is unity. The harmonic beam is polarized along x. The wave at 2ω is ordinary and perpendicular to the plane of incidence giving a transmission factor,

$$T_{2\omega}'' = \frac{2n_{2\omega}^0\cos\theta_{2\omega}'(\cos\theta + n_\omega^0\cos\theta_\omega')(n_\omega^0\cos\theta_\omega' + n_{2\omega}^0\cos\theta_{2\omega}')}{(n_{2\omega}^0\cos\theta_{2\omega}' + \cos\theta)^3}.$$

$\mathcal{R}$ is close to unity and can be assumed independent of θ. If we define the "normalized" Maker fringes as the ratio

$$P_N = P_{2\omega}''/P_M(0),$$

we can write

$$P_N = \frac{(n_\omega^0\cos\theta_\omega' + n_{2\omega}^0\cos\theta_{2\omega}')\cos^4\theta\cos\theta_{2\omega}'(n_\omega^0+1)^3(n_{2\omega}^0+1)^3}{(n_\omega^0\cos\theta_\omega' + \cos\theta)^3(n_{2\omega}^0\cos\theta_{2\omega}' + \cos\theta)^3(n_\omega^0 + n_{2\omega}^0)}\beta(\theta)\sin^2\Psi, \quad (21)$$

where

$$\Psi = (\pi L/2)(4/\lambda)(n_{2\omega}^0\cos\theta_\omega' - n_{2\omega}^0\cos\theta_{2\omega}').$$

(2) The input and output faces (010) of the sample are parallel to x and z. The sample is rotated about the optic axis z. The laser beam is polarized perpendicular to z. The fundamental wave is ordinary and parallel to the incidence plane.

$$t_\omega'(\theta)=2\cos\theta/(n_\omega^0\cos\theta+\cos\theta_\omega').$$

The relations between the crystal system (x, y, z) and the laboratory system (X, Y, Z) are

$$x=X \qquad y=Z \qquad z=-Y.$$

The nonlinear polarization is parallel to the plane of incidence. From Eq. (A42), we deduce $p_1=1$, $p_X=\cos2\theta_\omega'$, $p_Z=\sin2\theta_\omega'$, and from Eq. (A44) $p_2=\cos3\theta_\omega'$. The harmonic beam is polarized perpendicular to z and is an ordinary wave parallel to the plane of incidence for which the transmission factor $T_{2\omega}''$ is [see Eq. (12)]

$$T_{2\omega}''=\frac{2n_{2\omega}^0\cos\theta_{2\omega}'(n_\omega^0\cos\theta+\cos\theta_\omega')(n_{2\omega}^0\cos\theta_\omega'+n_\omega^0\cos\theta_{2\omega}')}{(\cos\theta_{2\omega}'+n_{2\omega}^0\cos\theta)^3}.$$

We get for the normalized Maker fringes

$$P_N=\frac{(n_{2\omega}^0\cos\theta_\omega'+n_\omega^0\cos\theta_{2\omega}')\cos^4\theta\cos\theta_{2\omega}'(n_{2\omega}^0+1)^3(n_{2\omega}^0+1)^3\cos^2(3\theta_\omega')}{(n_\omega^0\cos\theta+\cos\theta_\omega')^3(\cos\theta_{2\omega}'+n_{2\omega}^0\cos\theta)^3(n_\omega^0+n_{2\omega}^0)}\mathfrak{B}(\theta)\sin^2\Psi. \tag{22}$$

b. ADP, KDP Point Group $\bar{4}2m$. The nonlinear polarization is

$$\mathcal{P}_x=2d_{14}E_yE_z,$$

$$\mathcal{P}_y=2d_{14}E_zE_x,$$

$$\mathcal{P}_z=2d_{36}E_xE_y.$$

The input and output faces of the sample are (110). The sample is rotated about the optic axis z. The *laser beam* is polarized perpendicular to z, and is an ordinary wave, parallel to the plane of incidence whence

$$t_\omega'(\theta)=2\cos\theta/(n_\omega^0\cos\theta+\cos\theta_\omega').$$

The *nonlinear polarization* is parallel to z and perpendicular to the plane of incidence

$$p_1=2\cos[\theta_\omega'+(\pi/4)]\cos[\theta_\omega'-(\pi/4)],$$

$$p_2=1.$$

The *harmonic beam* is polarized along z, making it an extraordinary wave with wave vector parallel to the energy flow and perpendicular to the plane of incidence, whence

$$T_{2\omega}''=\frac{2n_{2\omega}^e\cos\theta_{2\omega}'(\cos\theta+n_\omega^0\cos\theta_\omega')(n_\omega^0\cos\theta_\omega'+n_{2\omega}^e\cos\theta_{2\omega}')}{(n_{2\omega}^e\cos\theta_{2\omega}'+\cos\theta)^3},$$

$$P_N=\frac{(n_\omega^0\cos\theta_\omega'+n_{2\omega}^e\cos\theta_{2\omega}')\cos^4\theta\cos\theta_{2\omega}'(n_\omega^0+1)^3(n_{2\omega}^e+1)^3(\cos\theta+n_\omega^0\cos\theta_\omega')}{(n_\omega^0\cos\theta+\cos\theta_\omega')^4(n_{2\omega}^e\cos\theta_{2\omega}'+\cos\theta)^3(n_\omega^0+n_{2\omega}^e)}$$

$$\times4\cos^2(\theta_\omega'+\pi/4)\cos^2(\theta_\omega'-\pi/4)\times\mathfrak{B}(\theta)\sin^2\Psi, \tag{23}$$

and

$$\Psi=(\pi L/2)(4/\lambda)(n_\omega^0\cos\theta_\omega'-n_{2\omega}^e\cos\theta_{2\omega}').$$

E. Comment on Effects of Spatial and Temporal Coherence of the Fundamental Laser Beam

The foregoing theory has been derived in the plane wave approximation for a strictly monochromatic fundamental laser beam. The inclusion of a finite beamwidth correction was made for a Gaussian beam. For comparison of experiment with the foregoing theory, one should therefore operate the laser in the lowest-order TEM_{00} mode. In addition the laser cavity length should be restricted so that only one longitudinal mode falls within the oscillating linewidth.

Relaxation of the second restriction introduces an additional multiplier into the transmitted second-harmonic power $\mathcal{P}_{2\omega}''$ given in Eqs. 14 and 15. This additional multiplier can be shown by an extension of the arguments given by Bloembergen[15] for normal incidence, to be independent of angle and hence does not affect the normalized envelope function P_N. The angular frequency differences between longitudinal modes are several orders-of-magnitude too small to give rise to a detectable difference in the refractive indices and the position of the Maker fringe minima is therefore the same for all the longitudinal modes.

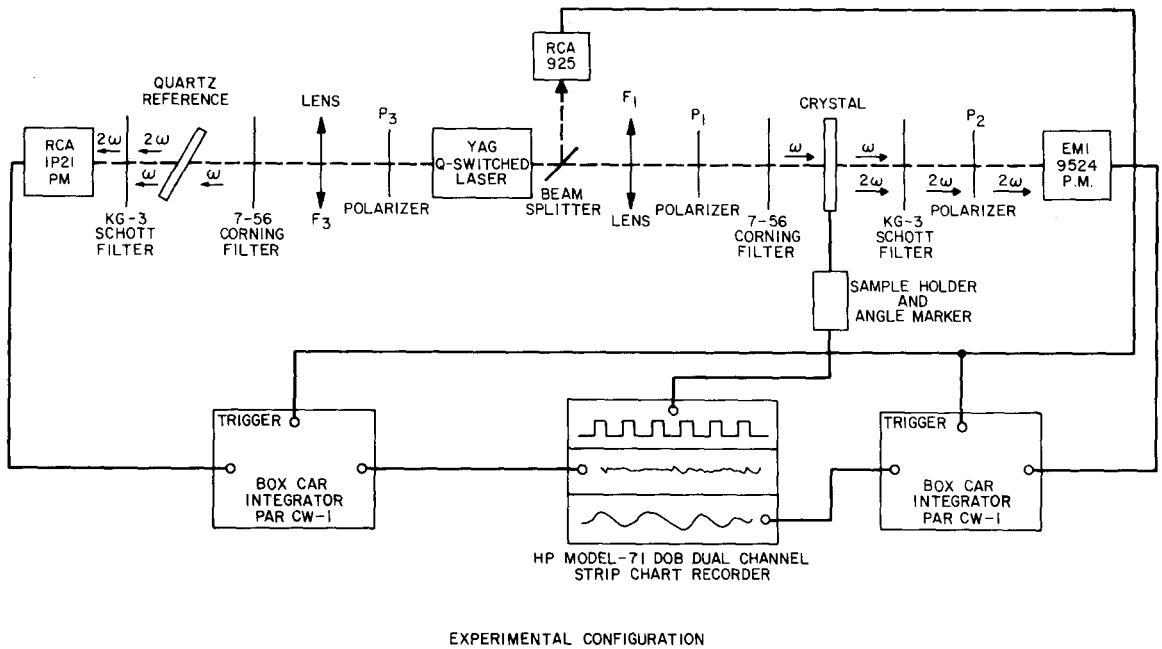

FIG. 2. Experimental configuration. The electrical connections are represented by continuous lines, light propagation by dashed lines.

The additional multiplier does affect $P_M(0)$ and has to be taken into account for absolute measurements of NLO coefficients. Because it is the same for all the NLO materials, it is without any influence on the relative NLO measurements.

III. EXPERIMENTAL RESULTS

A. Laser

The experiments were performed using a Nd:YAG laser. The output spectrum was analyzed using a monochrometer and was found to be a single line 0.6 cm^{-1} in width at 1064 nm.

The YAG rod (3.7-cm long and 2.5-mm diam) is mounted between two mirrors with 50-cm curvature radius, spaced 20-cm apart. The laser cavity is thus nearly confocal. Continuously pumped, the laser is Q switched by rotation of one mirror at a rate of 175 Hz. Peak powers are 1 kW with pulse widths of $\simeq$200 nsec. The beam has a small divergence with a measured half-angle of 1.5×10^{-3} rad which is within 15% of the theoretical value corresponding to a TEM_{00q} mode.

B. Experimental Arrangement

Represented in Fig. 2, the experimental configuration, except for a few modifications, is the same used by Kurtz and Perry,[16] Singh and Tipping.[17] The most important modification is the addition of a second-harmonic power reference system[6]: a quartz reference sample in an adjustable but fixed position corresponding to the first maximum of the Maker fringes.

In order to increase the second-harmonic power, the laser beam is focused by the lenses F_1 and F_3 with 25-cm and 4-cm focal length, respectively. It is necessary to have stronger focusing on the reference quartz sample because the laser power incident on it is much lower than that incident on the crystal being studied.

Two Glan–Thomson polarizers P_1 and P_3 are used to polarize the laser beam in such a way that the electric field is horizontal. The position of the analyzer P_2 and of the rotation axis (horizontal or vertical) depends on the crystal and on the nonlinear coefficient being measured. The rotation speed of the sample is adjustable in the range 1°–20° per minute. Low speed is used when the sample is thick or when the coherence length is short since Ψ is varying rapidly versus θ in these cases.

Both reference and signal are detected using a box car integrator with integrating time constant 1 msec and then recorded.

C. Experimental Procedure

According to the theoretical results, the Maker fringes have to be symmetric versus θ, with minima equal to zero. In order to get such features from the experimental data some care has to be taken with respect to the sample orientation and position versus the laser beam.

1. Nonzero Minima

In practice, the minima have values different from zero, a result which may come from several physical phenomena, of which the three most important are surface defects, beam divergence, and nonparallelism between the input and output faces of the sample. To avoid the first, the sample must be flat (to $\approx\lambda$) and free of scratches.

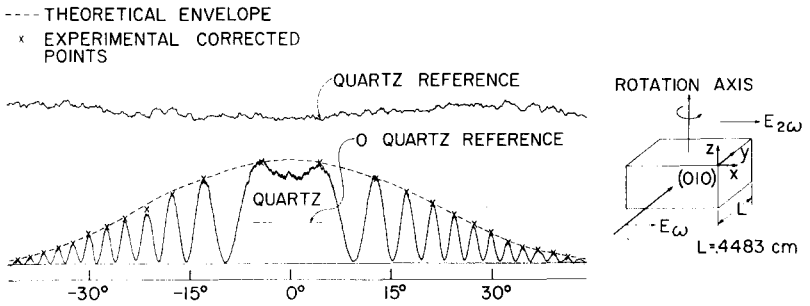

FIG. 3. Maker fringes for quartz (Fig. 3), ADP (Fig. 4), and KDP (Fig. 5), as a function of θ. The upper trace is the second harmonic produced by the reference quartz sample. To avoid any confusion between upper and lower trace, the zero line of the quartz reference has been shifted up. The experimental points indicated by crosses (x) have been corrected, taking into account the fluctuations of the quartz reference signal.

Let us evaluate the influence of the latter two effects.

a. Beam divergence. Near a minimum the harmonic power is, according to Eq. (15) $P_{2\omega}''=C\sin^2\Psi$, where C can be considered as a constant for small variations of θ. The measured power is in fact

$$\Delta P''=(2\Delta\theta)^{-1}\int_{\theta-\Delta\theta}^{\theta+\Delta\theta} C\sin^2\Psi d\theta$$

$$=C\tfrac{1}{3}(\Delta\theta)^2(d\Psi/d\theta)^2$$

averaged over the variation $2\Delta\theta$ for the angle of incidence. If ϵ is the beam divergence (half-angle) of the laser at the sample, the amplitude $\Delta P''$ of the minimum compared to the amplitude P'' of the next maximum is, for small values of θ

$$\Delta P''/P''=(\pi^2L^2/12n^4l_c^2)\epsilon^2\theta^2. \qquad (24)$$

Assuming $L=0.2$ cm, $l_c=10\ \mu m$, $n=1.5$, $\epsilon=3.10^{-3}$, we obtain $\Delta P''/P''=2\%$ at $\theta=30°$.

b. Wedge sample. The thickness L of the sample is not the same at the center of the beam and at the edges. If α is the angle between the input and output faces, w the spot radius of the beam, the value of the minimum averaged over L is

$$\Delta P''=(2w\alpha)^{-1}\int_{L-w}^{L+w} C\sin^2\Psi dL.$$

That means, by comparison with the amplitude P'' of the next maximum,

$$\Delta P''/P''=w^2\alpha^2\pi^2/12l_c^2. \qquad (25)$$

So we see the accuracy on the parallelism of the two sample faces must be greater when an unfocused laser beam is used. $\Delta P''/P''$ is less than 1% if the wedge angle α is lower than 20 min for $l_c=10\ \mu m$ and $w=200\ \mu m$.

In case of a nonzero minimum, the value of the next maximum can be corrected by adding the measured minimum $\Delta P''$ to the measured maximum:

$$P_{\text{meas}}''=P''[1-\tfrac{1}{3}(\Delta\theta)^2(d\Psi/d\theta)^2]=P''-\Delta P''.$$

2. Symmetry of the Fringes

It is necessary to position the crystal carefully to get symmetric fringes. The rotation axis must first be centered on the focused laser beam, perpendicular to it, at the beam waist. Otherwise, the fundamental power density incident on the crystal is not the same for $\theta>0$ and for $\theta<0$.

The plane of incidence must remain the same (horizontal or vertical) when the sample is rotated: The normal to the faces of the sample is adjusted perpendicular to the rotation axis.

Finally, the precise orientation of the crystallographic axes of the sample is checked: The rotation axis is generally parallel to one of the crystallographic axes. If this adjustment is not accurate, the projection factor $p(\theta)$ is asymmetric. This effect can be important for instance in the case of a quartz sample rotating about the optic axis.

All the positioning adjustments are made using a 632.8-nm He–Ne laser, which is colinear with the YAG laser. The crystallographic axis of the sample is oriented when extinction of the He–Ne laser light occurs with P_2 crossed to P_1 (Fig. 2).

D. Data Analysis

The data analysis is, for a given sample, divided in two parts: The first part involves determination of the coherence length or study of the function

$$\sin^2(\pi L/2)\,(4/\lambda)\,(n_\omega\cos\theta_\omega'-n_{2\omega}\cos\theta_{2\omega}')=\sin^2\Psi,$$

TABLE II. Experimental and computed positions of the fringe minima in quartz (010). L is the measured thickness of the sample, L' the thickness determined from the least-squares fit (see text).

$L=0.4483\pm0.0010$ cm; $L'=4477.5\ \mu$m

θ Exper.	θ Exper.	θ Theory
−9° 3/4	9° 1/2	9° 1/2
−15° 1/2	15° 1/4	15° 1/4
−19° 1/2	19° 1/2	19° 1/2
−23°	23°	22° 3/4
−26°	25° 3/4	25° 3/4
−28° 3/4	28° 1/2	28° 1/2
−31° 1/4	31° 1/4	31°
−33° 1/2	33° 1/2	33° 1/4
−35° 3/4	35° 3/4	35° 1/2
−38°	37° 1/2	37° 3/4
−39° 1/2	39° 1/2	39° 1/2

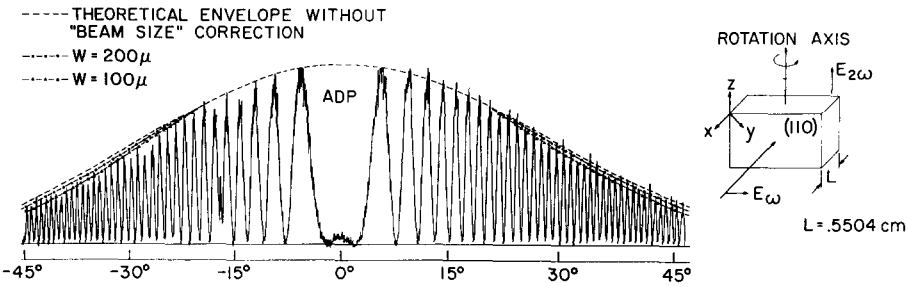

FIG. 4. Maker fringes for ADP. See Fig. 3.

and the second part involves comparison between the theoretical and experimental envelopes.

1. Coherence Length

For a definite λ, $\sin^2\Psi$ is a function of four variables: L, n_ω, $n_{2\omega}$ and θ. In fact $n_\omega - n_{2\omega}$ is along with θ the crucial variable for the period of the Maker fringes.

The comparison of theory and experiment is made by checking the self-consistency for the values of L, n_ω and $n_{2\omega}$ over the total range of variation for θ.

The positions of the minima are measured with a greater accuracy ($\leq \frac{1}{4}°$) than those of the maxima: There is no change in the position of the minimum if it does not go to zero while the positions of the maxima are affected by the laser fluctuations.

The experimental behavior of $\sin^2\Psi$ is therefore defined by the positions of all the minima and by the shape of the fringes at small angles θ. The theoretical behavior is computed and then compared with the experimental data.

(a) Assume that the refractive indices n_ω and $n_{2\omega}$ are well known (within a part in 10^{-4} or less). At normal incidence the value of $\sin^2\Psi$ is strongly dependent on the ratio L/l_c and the shape of the fringes near $\theta=0$ changes substantially for a small variation in L such as $\Delta L = l_c/5$ (less than 1 μm in some cases). Generally L is not known with a sufficient accuracy. So the value of L used in the computer program to find the theoretical variation of $\sin^2\Psi$ versus θ has to be adjusted in such a manner that the theory fits the experimental results for small values of θ.

The value of the coherence length itself is then verified by the fit for large values of θ (40° and above).

(b) n_ω and $n_{2\omega}$ are not well known (within 1 part in 10^{-3} or more).

The analysis in this case is a little more difficult. The values of L and $n_\omega - n_{2\omega}$ have to be alternately adjusted, L by considering the shape of the Maker fringes near $\theta=0$, and $n_\omega - n_{2\omega}$ by using the data for large values of θ.

The final fit indicates an accurate value of l_c, but the knowledge of n_ω and $n_{2\omega}$ separately is only slightly improved. Let us consider next the experimental data for quartz, ADP, and KDP.

Quartz. The value of the refractive index for the ordinary wave at 1064 nm is $n_\omega^0 = 1.53413$ and at 532.5 nm is $n_{2\omega}^0 = 1.54702$. The same coherence length $l_c = \lambda/4(n_{2\omega}^0 - n_\omega^0)$ is involved in the two experiments with orientation (011) and (010). We have measured the Maker fringes in two (011) samples with different thickness L and in one (010) sample. In Fig. 3 we show the Maker fringes for the (010) sample of thickness $L = 0.4483 \pm 0.0010$ cm. The theoretical computations indicated in Table II by comparison with experimental data have been made using $L' = 4477.5$ μm.

ADP. According to the data of Zernike[18] the ordinary refractive index at 1064 nm is $n_\omega^0 = 1.50663$ and for the extraordinary wave at 532.5 nm $n_{2\omega}^e = 1.48153$. Maker

TABLE III. Experimental and computed positions of the fringe minima in ADP (110). L and L' defined as in Table II (see text).

$L = 0.5504$ cm; $L' = 5507.8$ μm

θ Exper.	θ Exper.	θ Theory	θ Exper.	θ Exper.	θ Theory	θ Exper.	θ Exper.	θ Theory
−1° 3/4	1° 3/4	1° 3/4	−27° 1/4	27° 1/4	27° 1/4	−38° 1/2	38° 1/2	38° 1/2
−11°	10° 3/4	10° 3/4	−28°	28°	28° 1/4	−39°	39°	39°
−13° 1/4	13°	13° 1/4	−29° 1/4	29° 1/4	29° 1/4	−40°	40°	40° 1/4
−15° 1/4	15° 1/4	15° 1/4	−30°	30°	30°	−40° 3/4	40° 3/4	40° 3/4
	16° 3/4	17°	−31°	31°	31°	−41° 1/2	41° 1/4	41° 1/2
−18° 3/4	18° 1/2	18° 1/2	−32°	32°	32°	−42°	42° 1/4	42° 1/4
−20°	20°	20°	−33° 3/4	33° 3/4	33° 3/4	−42° 3/4	42° 3/4	42° 3/4
−21° 1/2	21° 1/4	21° 1/4	−34° 1/2	34° 1/2	34° 1/2	−43° 1/2	43° 1/2	43° 1/2
−22° 3/4	22° 1/2	22° 1/2	−35° 1/2	35° 1/4	35° 1/4	−44°	44° 1/4	44° 1/4
−24°	23° 3/4	23° 3/4	−36° 1/4	36°	36°	−44° 3/4	44° 3/4	45°
−25° 1/4	25°	25° 1/4	−37°	37°	37°			
−26° 1/4	26°	26° 1/4	−37° 3/4	37° 3/4	37° 3/4			

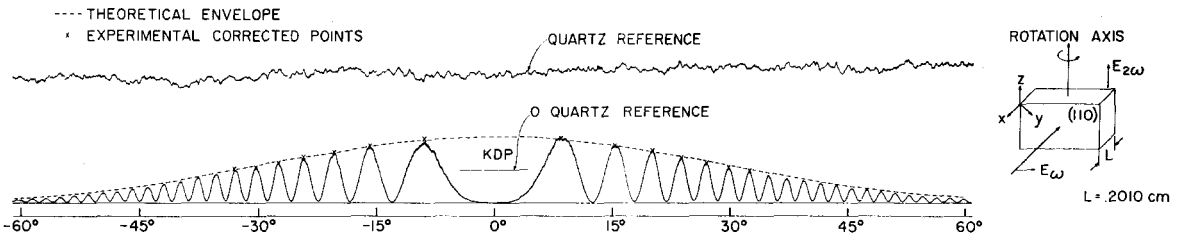

FIG. 5. Maker fringes for KDP. See Fig. 3.

fringes for two (110) samples of thickness $L=0.1666$ cm and $L=0.5504$ cm were measured. The results for the thicker sample are shown in Fig. 4 along with the analysis in Table III.

KDP. We measured two (110) samples and we represent in Fig. 5 one of the results ($L=0.201\pm 0.001$ cm). The theoretical computations of Table IV correspond to $L'=2011.6$ μm and the following values for the index of refraction[11]

$$n_\omega{}^0=1.49375, \qquad n_{2\omega}{}^e=1.47045.$$

For the three materials, agreement between experimental minima and theoretical values is within the accuracy, $\Delta\theta\leq\frac{1}{4}°$, of the experimental data.

To evaluate the corresponding accuracy on the experimental value of the coherence length l_c, we computed the Maker fringes for a given thickness with a variation of 1% in the difference $n_\omega-n_{2\omega}$.

It turns out that a change of 1% for l_c produces *a shift for all the minima positions* of 1/2° in the range $35°\leq\theta\leq 50°$. Under these conditions the accuracy of the measured coherence length is *greater than* 1% and the experimental values are

$$\text{Quartz } l_c=20.65\ \mu\text{m}\pm 0.05\ \mu\text{m},$$
$$\text{ADP } l_c=10.59\ \mu\text{m}\pm 0.02\ \mu\text{m},$$
$$\text{KDP } l_c=11.43\ \mu\text{m}\pm 0.02\ \mu\text{m}.$$

2. *Envelope*

The amplitudes of the maxima can be affected by variations in the laser power. It is therefore necessary to correct the peaks, with respect to the quartz reference, for such power fluctuations. In the case of nonzero minimum another correction must be made on the next peak: The real peak value, measured from the 0 level, is equal to the recorded value increased by the value of the minimum, according to the results of Sec. III.C.

The corrected experimental data are to be compared with the computed theoretical values, using the normalized envelope given, for each case, by one of the Eqs. (21)–(23). The amplitudes and the positions of the maxima are the input data of a least-squares curve fitting computer program which determines $P_M(0)$ and the rms error $\Delta P_M(0)$. The theoretical computed envelope is then plotted and compared with the experimental data, as shown in Figs. 3–5.

The theoretical envelope fits the experimental data very well, except on Fig. 4, i.e., in the case of a thick ADP sample. A better fit can be obtained for these fringes if the "beam size correction" is taken into account. The corrected envelopes were plotted for the two values of w: 100 and 200 μm. We can see that the equivalent Gaussian spot radius of the laser is about 150 μm in agreement with the value deduced from direct measurements (variation of the photographed beam size when the laser is attenuated by calibrated filters). The beam size correction is negligible in all other samples because the thickness is smaller and, in addition for the quartz, the dispersion $n_\omega-n_{2\omega}$ is low.

Because the signal to noise ratio is decreasing at large values of θ we computed $P_M(0)$ and the rms error $\Delta P_M(0)$ for three sets of data corresponding to the

TABLE IV. Experimental and computed positions of the fringe minima in KDP (110). L and L' as defined in Table II (see text).

$L=0.201$ cm; $L'=2011.6$ μm					
θ Exper.	θ Exper.	θ Theory	θ Exper.	θ Exper.	θ Theory
−12° 3/4	12° 3/4	12° 3/4	−36° 1/2	36° 1/4	36° 1/2
−18° 1/4	18°	18°	−38° 3/4	38° 1/2	38° 3/4
−22° 1/4	22°	22°	−40° 3/4	40° 3/4	40° 1/2
−25° 1/2	25° 1/2	25° 1/2	−42° 3/4	42° 1/2	42° 1/2
−28° 1/2	28° 1/2	28° 1/2	−44° 3/4	44° 1/2	44° 3/4
−31° 1/2	31° 1/4	31° 1/2	−46° 3/4	46° 1/2	46° 1/2
−34°	33° 3/4	33° 3/4	−48° 1/2	48° 1/2	48° 1/2

same crystal:

(1) maxima in the range $|\theta| \leq 30°$,
(2) maxima in the range $|\theta| \leq 45°$,
(3) all the maxima.

For example, in the case of quartz (Fig. 3) the results are

$$\begin{array}{llll} |\theta| \leq 30° & P_M(0) = 3.79 & \Delta P_M(0) = 0.13 \\ |\theta| \leq 45° & P_M(0) = 3.80 & \Delta P_M(0) = 0.12 \\ |\theta| \leq 62° & P_M(0) = 3.77 & \Delta P_M(0) = 0.12. \end{array}$$

This demonstrates that the theory fits the experimental envelope and that it is possible to deduce an accurate value of $P_M(0)$ by considering only the maxima in the range $|\theta| \leq 30°$.

For all the crystals studied the rms error $\Delta P_M(0)$ was less than 5% of $P_M(0)$.

IV. CONCLUSION

A complete theory of Maker fringes in nonabsorbing isotropic and uniaxial crystals has been derived which includes all the corrections necessary for making precise determinations of nonlinear optical coefficients. These corrections include finite beamwidth effects and multiple reflections corrections. Comparison of this theory with extensive experimental data on the Maker fringes in quartz, ADP, and KDP shows agreement to within the experimental accuracy of about 5% on the Maker fringe envelopes and to better than 1% on the coherence lengths. We conclude from this study that a careful analysis of Maker fringes can yield precise values of the nonlinear optical coefficients and coherence lengths in isotropic and uniaxial crystals. This is of great importance in establishing *accurate* and *reliable* standards in the field of nonlinear optics.

ACKNOWLEDGMENTS

We would like to thank R. C. Miller for suggesting this work. It is a pleasure to acknowledge many helpful discussions with J. A. Giordmaine, S. Singh, and I. Freund. S. Singh kindly provided the (010) quartz sample. The technical assistance of T. T. Perry has been appreciated.

APPENDIX A: SOLUTION OF MAXWELL'S EQUATIONS INCLUDING BOUNDARY CONDITIONS

In a nonlinear material, the constitutive relation between the electric induction $\mathbf{D}$ and the electric field $\mathbf{E}$ must include the existence of a nonlinear polarization[1]

$$\begin{aligned} \mathcal{P}_{2\omega}'(\mathbf{r}, t) &= \hat{p}\mathcal{P}_{2\omega}'(\mathbf{r}, t) \\ &= \tfrac{1}{2}[\mathcal{P}_{2\omega}' \exp(i\mathbf{k}\cdot\mathbf{r}) \exp(-i\omega t) + \text{c.c.}], \end{aligned} \quad \text{(A1)}$$

where $\hat{p}$ is a unit vector in the direction of the nonlinear polarization and the amplitude $\mathcal{P}_{2\omega}'$ is independent of time. This amplitude is in turn related to the electric field amplitude $\mathbf{E}_\omega'$ through the NLO tensor $\mathbf{d}$ by the basic relation

$$\mathcal{P}_{2\omega}' = \mathbf{d} : \mathbf{E}_\omega' \otimes \mathbf{E}_\omega',$$

where $\mathbf{E}_\omega' \otimes \mathbf{E}_\omega'$ is the direct product of the vector $\mathbf{E}_\omega'$ by itself.

This nonlinear polarization acts as a source term in the wave equation[5]

$$\begin{aligned} \nabla \times \nabla \times \mathbf{E}_{2\omega}'(\mathbf{r}, t) + (n_{2\omega}^2/c^2)[\partial^2 \mathbf{E}_{2\omega}'(\mathbf{r}, t)/\partial t^2] \\ = -(4\pi/c^2)[\partial^2 \mathcal{P}_{2\omega}'(r, t)/\partial t^2]. \end{aligned} \quad \text{(A2)}$$

The solution of the wave equation (A2) for the electric field can be written as follows[5]:

$$\begin{aligned} \mathbf{E}_{2\omega}' = \hat{e}_f R_f' \exp(i\mathbf{k}_f\cdot\mathbf{r}) + [4\pi\mathcal{P}_{2\omega}'/(n_\omega^2 - n_{2\omega}^2)] \\ \times [\hat{p} - \mathbf{k}_b(\mathbf{k}_b\cdot\hat{p})/|k_f|^2] \exp(i\mathbf{k}_b\cdot\mathbf{r}). \end{aligned} \quad \text{(A3)}$$

The first term of (A3) is the "free wave" solution of (A2) when $\mathcal{P}_{2\omega}' = 0$, and the second term is the "bound wave," a particular solution of (A2). $\hat{e}_f$ is a unit vector, $\mathbf{k}_f$ and $\mathbf{k}_b$ are the wave vectors for the free and bound waves, respectively. The magnetic field is

$$\begin{aligned} \mathbf{H}_{2\omega}' = (c/2\omega)(\mathbf{k}_f \times \hat{e}_f) E_f' \exp(i\mathbf{k}_f\cdot\mathbf{r}) \\ + [4\pi\mathcal{P}_{2\omega}'/(n_\omega^2 - n_{2\omega}^2)]\cdot(c/2\omega)(\mathbf{k}_b \times \hat{p}) \exp(i\mathbf{k}_b\cdot\mathbf{r}). \end{aligned} \quad \text{(A4)}$$

A. Boundary Conditions at $Z = 0$

Because of the presence of a source term in Eq. (A2) there is a reflected-harmonic wave in air at the input face of the crystal

$$\mathbf{E}_{2\omega}^R = \hat{e}_R E_R \exp(i\mathbf{k}_2^R\cdot\mathbf{r}), \quad \text{(A5)}$$

$$\mathbf{H}_{2\omega}^R = (c/2\omega)(\mathbf{k}_2^R \times \hat{e}_R) E_R \exp(i\mathbf{k}_2^R\cdot\mathbf{r}). \quad \text{(A6)}$$

$\mathbf{k}_f$, $\mathbf{k}_b$, $\mathbf{k}_2^R$, $\hat{e}_f$, $\hat{e}_R$, E_f', and E_R have to be determined from the boundary conditions at the input face of the crystal, i.e., continuity for the tangential components of the electric and magnetic fields.

The fact that these tangential components should be continuous everywhere on the boundary at all times leads first to the determination of $\mathbf{k}_f$, $\mathbf{k}_b$ and $\mathbf{k}_2^R$. For $\mathbf{k}_f$ and $\mathbf{k}_b$ the result is as indicated by the Eqs. (6)–(9). For $\mathbf{k}_2^R$

$$\theta^R = -\theta,$$

$$|\mathbf{k}_2^R| = 2\omega/c.$$

Let us now calculate $\hat{e}_f$, $\hat{e}_R$, E_f', and E_R. In order to simplify the mathematical manipulations, let us take

$$\hat{e}_b = \hat{p} - [\mathbf{k}_b(\mathbf{k}_b\cdot\hat{p})/|k_f|^2] \quad \text{(A7)}$$

$$Q' = 4\pi\mathcal{P}_{2\omega}'/(n_\omega^2 - n_{2\omega}^2). \quad \text{(A8)}$$

At $\mathbf{r} = 0$, Eqs. (A3)–(A6) are

$$\mathbf{E}_{2\omega}' = \hat{e}_f E_f' + \hat{e}_b Q', \quad \text{(A9)}$$

$$\mathbf{H}_{2\omega}' = (c/2\omega)(\hat{k}_f \times \hat{e}_f) E_f' + Q'(c/2\omega)(\mathbf{k}_b \times \hat{p}), \quad \text{(A10)}$$

$$\mathbf{E}_{2\omega}^R = \hat{e}_R E_R, \quad \text{(A11)}$$

$$\mathbf{H}_{2\omega}^R = (c/2\omega)(\mathbf{k}_R \times \hat{e}_R) E_R. \quad \text{(A12)}$$

According to the coordinate system (X, Y, Z) indicated on Fig. 1, the continuity relations are

$$\hat{X}\cdot\hat{e}_R E_R=\hat{X}\cdot\hat{e}_f E_f'+\hat{X}\cdot\hat{e}_b Q', \quad \text{(A13)}$$

$$(\mathbf{k}_R\times\hat{e}_R)\cdot\hat{X}E_R=\hat{X}\cdot(\mathbf{k}_f\times\hat{e}_f)E_f'+\hat{X}\cdot(\mathbf{k}_b\times\hat{p})Q', \quad \text{(A14)}$$

$$\hat{Y}\cdot\hat{e}_R E_R=\hat{Y}\cdot\hat{e}_f E_f'+\hat{Y}\cdot\hat{e}_b Q', \quad \text{(A15)}$$

$$(\mathbf{k}_R\times\hat{e}_R)\cdot\hat{Y}E_R=Y\cdot(\mathbf{k}_f\times\hat{e}_f)E_f'+\hat{Y}\cdot(\mathbf{k}_b\times\hat{p})Q'. \quad \text{(A16)}$$

Let us consider the projections on X, Y, Z of $\hat{e}_b$, $\hat{e}_f$, $\hat{e}_R$, and $\hat{p}$

	$\hat{e}_b$	$\hat{e}_f$	$\hat{e}_R$	$\hat{p}$
X	b_X	f_X	R_X	p_X
Y	b_Y	f_Y	R_Y	p_Y
Z	b_Z	f_Z	R_Z	p_Z.

Equations (A13)–(A16) become

$$R_X E_R=f_X E_f'+b_X Q', \quad \text{(A17)}$$

$$R_Y k_{RZ}E_R=f_Y k_{fZ}E_f'+b_Y k_{bZ}Q', \quad \text{(A18)}$$

$$R_Y E_R=f_Y k_{fZ}E_f'+p_Y k_{bZ}Q', \quad \text{(A19)}$$

$$(R_X k_{RZ}-R_Z k_{RX})E_R=(f_X k_{fZ}-f_Z k_{fX})E_f'+(p_X k_{bZ}-p_Z k_{bX})Q'. \quad \text{(A20)}$$

1. The nonlinear polarization is perpendicular to the plane of incidence:

$$p_X=p_Z=0, \qquad p_Y=1,$$

$$\mathbf{k}_b\cdot\hat{p}=0.$$

Then $\hat{e}_b=\hat{p}$ and $b_Y=1$. The continuity relations are

$$R_X E_R=f_X E_f', \quad \text{(A21)}$$

$$(R_X k_{RZ}-R_Z k_{RX})E_R=(f_X k_{fZ}-f_Z k_{fX})E_f', \quad \text{(A22)}$$

$$R_Y E_R=f_Y E_f'+Q', \quad \text{(A23)}$$

$$R_Y k_{RZ}E_R=f_Y k_{fZ}E_f'+k_{bZ}Q'. \quad \text{(A24)}$$

(A21) and (A22) are independent of Q' and exactly the same as in the case in which there is no second-order polarization, i.e., no field at 2ω. We deduce $R_X=f_X=0=R_Z=f_Z$. (A23) and (A24) lead to

$$E_R=E_f'+Q',$$

$$n_{2\omega}\cos\theta_{2\omega}'E_f'+n_\omega\cos\theta_\omega'Q'=-\cos\theta E_R,$$

or

$$E_f'=-Q'\frac{\cos\theta+n_\omega\cos\theta_\omega'}{n_{2\omega}\cos\theta_{2\omega}'+\cos\theta}. \quad \text{(A25)}$$

We can now rewrite (A3) as follows:

$$\mathbf{E}_{2\omega}'=\hat{Y}Q'\left(-\frac{\cos\theta+n_\omega\cos\theta_\omega'}{n_{2\omega}\cos\theta_{2\omega}'+\cos\theta}\times\exp(i\mathbf{k}_f\cdot\mathbf{r})+\exp(i\mathbf{k}_b\cdot\mathbf{r})\right). \quad \text{(A26)}$$

2. The nonlinear polarization is in the plane of incidence:

$$p_Y=0,$$

$$b_X=p_X-(n_\omega^2/n_{2\omega}^2)\sin\theta_\omega'(\sin\theta_\omega'p_X+\cos\theta_\omega'p_Z),$$

$$b_Y=0,$$

$$b_Z=p_Z-(n_\omega^2/n_{2\omega}^2)\cos\theta_\omega'(\sin\theta_\omega'p_X+\cos\theta_\omega'p_Z).$$

Equations (A13)–(A16) become

$$R_X E_R=f_X E_f'+b_X Q', \quad \text{(A27)}$$

$$(f_X k_{fZ}-f_Z k_{fX})E_f'+Q'(p_X k_{bZ}-p_Z k_{bX})=(R_X k_{RZ}-R_Z k_{RX})E_R, \quad \text{(A28)}$$

$$R_Y E_R=f_Y E_f', \quad \text{(A29)}$$

$$R_Y k_{RZ}E_R=f_Y k_{fZ}E_f'. \quad \text{(A30)}$$

Equations (A29) and (A30) give the result

$$R_Y=f_Y=0$$

and we can write the continuity relation as

$$-E_R\cos\theta=E_f'\cos\theta_{2\omega}'+b_X Q',$$

$$E_R=n_{2\omega}E_f'+n_\omega Q'(p_X\cos\theta_\omega'-p_Z\sin\theta_\omega'),$$

which leads to

$$E_f'=-Q'\frac{b_X+n_\omega\cos\theta(p_X\cos\theta_\omega'-p_Z\sin\theta_\omega')}{\cos\theta_{2\omega}'+n_{2\omega}\cos\theta}=-\beta Q'. \quad \text{(A31)}$$

Using in (A3) the value of E_f' coming from (A31) we get

$$\mathbf{E}_{2\omega}'=-\hat{e}_f\beta Q'\exp(i\mathbf{k}_f\cdot\mathbf{r})+\hat{e}_b Q'\exp(i\mathbf{k}_b\cdot\mathbf{r}). \quad \text{(A32)}$$

B. Boundary Conditions at $Z=L$

At the output face of the sample the bound and free waves are transmitted in air and produce a free wave $\mathbf{E}_{2\omega}''$ with the wave vector $\mathbf{k}_{2\omega}''$

$$\mathbf{k}_{2\omega}''=2\mathbf{k}_\omega.$$

So long as the reflections of $\mathbf{E}_\omega'$ at $Z=L$ are neglected, there is no reflected bound wave. The reflected free wave at 2ω is $\mathbf{E}_f'^R$ with the wave vector $\mathbf{k}_f'^R$

$$\theta_f'^R=-\theta_{2\omega}',$$

$$|\mathbf{k}_f'^R|=n_{2\omega}'(2\omega/c).$$

1. The nonlinear polarization is perpendicular to the plane of incidence: Because of the continuity conditions for the tangential components of the wave vectors, the continuity relations for the electric fields and the

magnetic fields are

$$E_f' \exp(i\mathbf{k}_f\cdot\hat{Z}L)+Q' \exp(i\mathbf{k}_b\cdot\hat{Z}L)+E_f'^R \exp(-i\mathbf{k}_f\cdot\hat{Z}L)=E_{2\omega}'' \exp(2i\mathbf{k}_\omega\cdot ZL), \tag{A33}$$

$$-n_{2\omega}\cos\theta_{2\omega}'E_f \exp(i\mathbf{k}_f\cdot\hat{Z}L)-n_\omega\cos\theta_\omega'Q' \exp(i\mathbf{k}_b\cdot\hat{Z}L)+n_{2\omega}\cos\theta_{2\omega}'E_f'^R \exp(-i\mathbf{k}_f\cdot\hat{Z}L)$$
$$=-\cos\theta E_{2\omega}'' \exp(2i\mathbf{k}_\omega\cdot\hat{Z}L). \tag{A34}$$

Eliminating $E_f'^R$ between (A33) and (A34), we calculate $E_{2\omega}''$

$$E_{2\omega}'' \exp(2i\mathbf{k}_\omega\cdot\hat{Z}L)=\frac{2n_{2\omega}\cos\theta_{2\omega}'}{\cos\theta+n_{2\omega}\cos\theta_{2\omega}'}E_f' \exp(i\mathbf{k}_f\cdot\hat{Z}L)+\frac{n_\omega\cos\theta_\omega'+n_{2\omega}\cos\theta_{2\omega}'}{\cos\theta+n_{2\omega}\cos\theta_{2\omega}'}Q' \exp(i\mathbf{k}_b\cdot\hat{Z}L), \tag{A35}$$

and the intensity $I_{2\omega}''$ of the second-harmonic beam coming out of the crystal is

$$I_{2\omega}''=(c/8\pi)\mathbf{E}_{2\omega}''\times\mathbf{H}_{2\omega}''^*=(c/8\pi)\mid E_{2\omega}''\mid^2.$$

Using (A8) and (A25),

$$I_{2\omega}''=\frac{c}{8\pi}\frac{16\pi^2\mid\mathcal{P}_{2\omega}'\mid^2}{(n_\omega^2-n_{2\omega}^2)^2}\left(8n_{2\omega}\cos\theta_{2\omega}'\frac{(\cos\theta+n_\omega\cos\theta_\omega')(n_\omega\cos\theta_\omega'+n_{2\omega}\cos\theta_{2\omega}')}{(n_{2\omega}\cos\theta_{2\omega}'+\cos\theta)^3}\sin^2\Psi\right.$$
$$\left.+\frac{(n_\omega\cos\theta_\omega'-n_{2\omega}\cos\theta_{2\omega}')^2}{(n_{2\omega}\cos\theta_{2\omega}'+\cos\theta)^4}(n_{2\omega}\cos\theta_{2\omega}'-\cos\theta)^2\right), \tag{A36}$$

where

$$\Psi=(\pi L/2)(4/\lambda)(n_\omega\cos\theta_\omega'-n_{2\omega}\cos\theta_{2\omega}').$$

The second component of $I_{2\omega}''$ in Eq. (A36) is independent of L and does not exhibit an oscillatory behavior. Its amplitude is several orders-of-magnitude smaller than the maximum of the first term. It can generally be neglected.

2. The nonlinear polarization is in the plane of incidence: The continuity relations are

$$\cos\theta_{2\omega}'E_f' \exp(i\mathbf{k}_f\cdot\hat{Z}L)+b_XQ' \exp(i\mathbf{k}_b\cdot\hat{Z}L)-\cos\theta_{2\omega}'E_f'^R \exp(-i\mathbf{k}_f\cdot\hat{Z}L)=\cos\theta E_{2\omega}'' \exp(2i\mathbf{k}_\omega\cdot\hat{Z}L), \tag{A37}$$

$$n_{2\omega}E_f' \exp(i\mathbf{k}_f\cdot\hat{Z}L)+n_\omega Q'(\cos\theta_\omega'p_X-\sin\theta_\omega'p_Z) \exp(i\mathbf{k}_b\cdot\hat{Z}L)+n_{2\omega}E_f'^R \exp(-i\mathbf{k}_f\cdot\hat{Z}L)=E_{2\omega}'' \exp(2i\mathbf{k}_\omega\cdot\hat{Z}L). \tag{A38}$$

From (A37) and (A38) we deduce

$$E_{2\omega}'' \exp(2i\mathbf{k}_\omega\cdot\hat{Z}L)=\frac{2n_{2\omega}\cos\theta_{2\omega}'}{n_{2\omega}\cos\theta+\cos\theta_{2\omega}'}E_f' \exp(i\mathbf{k}_f\cdot\hat{Z}L)+\frac{n_{2\omega}b_X+n_\omega\cos\theta_{2\omega}'(\cos\theta_\omega'p_X-\sin\theta_\omega'p_Z)}{n_{2\omega}\cos\theta+\cos\theta_{2\omega}'}Q' \exp(i\mathbf{k}_b\cdot\hat{Z}L).$$

The intensity $I_{2\omega}''$ is, using (A8) and (A31),

$$I_{2\omega}''=\frac{c}{8\pi}\frac{16\pi^2\mid\mathcal{P}_{2\omega}'\mid^2}{(n_\omega^2-n_{2\omega}^2)^2}\left\{8n_{2\omega}\cos\theta_{2\omega}'\frac{[b_x+n_\omega\cos\theta(p_X\cos\theta_\omega'-p_Z\sin\theta_\omega')][n_{2\omega}b_X+n_\omega\cos\theta_{2\omega}'(\cos\theta_\omega'p_x-\sin\theta_\omega'p_Z)]}{(n_{2\omega}\cos\theta+\cos\theta_{2\omega}')^3}\right.$$
$$\left.\times\sin^2\Psi+\left[\frac{2\beta n_{2\omega}\cos\theta_{2\omega}'}{n_{2\omega}\cos\theta+\cos\theta_{2\omega}'}-\left(\frac{n_{2\omega}b_X+n_\omega\cos\theta_{2\omega}'(\cos\theta_\omega'p_X-\sin\theta_\omega'p_Z)}{(n_{2\omega}\cos\theta+\cos\theta_{2\omega}')^2}\right)\right]^2\right\}. \tag{A39}$$

As before, we neglect the second component of $I_{2\omega}''$. Let us consider the term

$$\cos\theta_\omega'(p_X\cos\theta_\omega'-p_Z\sin\theta_\omega')=p_X-\sin\theta_\omega'(p_X\sin\theta_\omega'+\cos\theta_\omega'p_Z).$$

From previous calculations we found

$$b_X=p_X-(n_\omega^2/n_{2\omega}^2)\sin\theta_\omega'(p_X\sin\theta_\omega'+\cos\theta_\omega'p_Z).$$

Combining these two results we see that for materials in which the dispersion is not very important (i.e., $n_\omega\simeq n_{2\omega}$) and for $\mid\theta\mid\leq\pi/4$, it is possible to write

$$b_X\simeq\cos\theta_\omega'(p_X\cos\theta_\omega'-p_Z\sin\theta_\omega').$$

If η is the angle $(\hat{p},\hat{x})$, $I_{2\omega}''$ can be written as

$$I_{2\omega}''=\frac{c}{8\pi}\frac{16\pi^2\mid\mathcal{P}_{2\omega}'\mid^2}{(n_\omega^2-n_{2\omega}^2)^2}8n_{2\omega}\cos\theta_{2\omega}'\cos^2(\theta_\omega'-\eta)\frac{(n_\omega\cos\theta+\cos\theta_\omega')(n_{2\omega}\cos\theta_\omega'+n_\omega\cos\theta_{2\omega}')}{(n_{2\omega}\cos\theta+\cos\theta_{2\omega}')^3}\sin^2\Psi. \tag{A40}$$

In summary, we deduce from the formulas (A1), (A36), and (A40) the following relation between the second-

harmonic power density $I_{2\omega}''$ and $\mathbf{E}_\omega'$

$$I_{2\omega}''=[8\pi c/(n_\omega^2-n_{2\omega}^2)^2]d^2p^2(\theta)\mid E_\omega'\mid^4 T_{2\omega}''\sin^2[(\pi L/2)(4/\lambda)(n_\omega\cos\theta_\omega'-n_{2\omega}\cos\theta_{2\omega}')], \tag{A41}$$

where d is the NLO coefficient involved in the experiment and $p(\theta)$ is the "projection factor." $p(\theta)$ is the product of two quantities p_1 and p_2, i.e., $p(\theta)=p_1p_2$.

p_1 comes from (A1) written in terms of amplitudes

$$\mid \mathcal{P}_{2\omega}'\mid=\mid \mathbf{d}\mathbf{E}_\omega'\otimes\mathbf{E}_\omega'\mid=p_1d\mid \mathbf{E}_\omega'\mid^2. \tag{A42}$$

If the nonlinear polarization $\mathcal{P}_{2\omega}'$ is perpendicular to the plane of incidence

$$p_2=1,$$

$$T_{2\omega}''=2n_{2\omega}\cos\theta_{2\omega}'\frac{(\cos\theta+n_\omega\cos\theta_\omega')(n_\omega\cos\theta_\omega'+n_{2\omega}\cos\theta_{2\omega}')}{(n_{2\omega}\cos\theta_{2\omega}'+\cos\theta)^3}. \tag{A43}$$

For a nonlinear polarization in the plane of incidence

$$p_2=\cos(\theta_\omega'-\eta), \tag{A44}$$

$$T_{2\omega}''=2n_{2\omega}\cos\theta_{2\omega}'\frac{(n_\omega\cos\theta+\cos\theta_\omega')(n_{2\omega}\cos\theta_\omega'+n_\omega\cos\theta_{2\omega}')}{(n_{2\omega}\cos\theta+\cos\theta_{2\omega}')^3}. \tag{A45}$$

APPENDIX B: MULTIPLE REFLECTIONS CORRECTION

We have assumed, so far, that in the crystal the fundamental and harmonic waves are traveling from $Z=0$ to $Z=L$ (forward direction), without waves in the reverse direction. This assumption is a first-order approximation because at the boundaries $Z=0$ and $Z=L$ the waves are reflected. This induces a change in the amplitude of the forward waves, and the backward waves can no longer be ignored.

The solution of this problem can be obtained in the following way: Taking into account the multiple reflections of the fundamental wave, the forward $\mathbf{E}_\omega'$ and backward $\mathbf{E}_\omega'^R$ can be calculated. The nonlinear polarization is then deduced from

$$\mathcal{P}_{2\omega}'=\mathbf{d}(\mathbf{E}_\omega'+\mathbf{E}_\omega'^R)\otimes(\mathbf{E}_\omega'+\mathbf{E}_\omega'^R) \tag{B1}$$

and introduced as a source term in the wave equation at 2ω. Using the same method as in Appendix A, the electric field at 2ω is decomposed in a sum of bound and free waves where orientations, amplitude, and phase are determined by the boundary conditions at both faces of the crystal. This leads to very complex formulas of the same kind as those given by Bloembergen and Pershan for the nonlinear plane-parallel plate.[5] These formulas, besides the fact that they hardly can be used by the experimentalist, do not describe the multiple reflection phenomenon as it usually occurs. To make this point clear let us consider the plane-parallel slab in the linear case, i.e., without any second-harmonic generation. If t and r are the transmission and reflection coefficients given by Fresnel's formulas, the complex amplitude of the electric field transmitted in air at $Z=L$, after m multiple reflections is

$$E_m=Et^2r^{2m}\exp(2imk_z'L),$$

where E is the complex amplitude of the incoming beam and k_z' the Z component of the wave vector inside the crystal.

The intensity J of the transmitted beam can be written as

$$J\propto\sum_{m,p}E_mE_p^*=\sum_m\mid E_m\mid^2+\sum_{m\neq p}E_mE_p^*. \tag{B2}$$

In the ideal case where the two faces of the sample are strictly parallel we get

$$J=[t^4/(1+r^4-2r^2\cos2k_z'L)]I. \tag{B3}$$

I is the intensity of the incoming beam. The transmission of the slab is an oscillating function of L, i.e., the slab acts as an interferometer. More generally the crystal faces are not flat and parallel enough to get a constant phase difference $\exp(2ik_z'L)$ between E_m and E_{m+1}. An upper limit on the variation ΔL for which (B3) is valid can be obtained from the condition

$$2k_z'\Delta L\leq\pi/2$$

which leads to

$$\Delta L<\lambda/8n\simeq0.1\mu\text{m}$$

or less. If $\Delta L\geq\lambda/8$ we deduce from (B2)

$$J=[t^4I/(1-r^4)]+t^4I\sum_{m\neq p}r^{2(m+p)}\cos\delta \tag{B4}$$

with random values for δ. The transmission factor is therefore

$$J/I=t^4/(1-r^4), \tag{B5}$$

independant of L_1 because the fields E_m and E_p are incoherent. Let us come back now to the "nonlinear" case. *We assume the crystal sample is a plane-parallel slab but not an interferometer.*

In these conditions we are allowed to consider, at a given frequency and for a given kind of wave (free or bound), that the consecutive fields E_m are incoherent.

Nevertheless, the flatness of the faces is sufficient to provide, at the output face $Z=L$, a constant phase difference $\exp i(\mathbf{k}_b-\mathbf{k}_f)\cdot\hat{Z}L$ between the free and bound harmonic waves with the *same* index m.

An upper limit of the random variations ΔL is

$$(2\omega/c)\,(n_{2\omega}-n_\omega)\,\Delta L<\pi/2$$

or $\Delta L<l_c/2$; a quite obvious result. The factor

$$\sin^2\Psi=\sin^2[(\pi L/2)\,(4/\lambda)\,(n_\omega\cos\theta_\omega'-n_{2\omega}\cos\theta_{2\omega}')]$$

is therefore the same for all the transmitted harmonic waves, which are incoherent. Thus the multiple reflections correction $\mathfrak{R}$ affects only the envelope of the Maker fringes.

To calculate $\mathfrak{R}$ we proceed in the following sequence:

(1) Sum multiple reflections of the second-harmonic light generated by the first forward pass of the laser beam.

(2) Sum multiple reflections of the second-harmonic light generated by the first backward pass of the laser.

(3) Sum multiple reflections of the second-harmonic light generated by the second forward pass of the laser. And so on $\cdots$.

r_ω is the reflection coefficient for the fundamental wave and $r_{2\omega}$ for the harmonic waves (because θ_ω' and $\theta_{2\omega}'$ are nearly equal, we can assume the same value of the reflection coefficient for the free and bound waves at 2ω).

First Forward Pass

$$E_{2\omega,0}'' \qquad P_{2\omega,0}''$$

$$E_{2\omega,1}''=r_{2\omega}^2E_{2\omega,0}'' \qquad P_{2\omega,1}''=r_{2\omega}^4P_{2\omega,0}''$$

$$E_{2\omega,2}''=r_{2\omega}^4E_{2\omega,0}'' \qquad P_{2\omega,2}''=r_{2\omega}^8P_{2\omega,0}''$$

$$P_{2\omega}''^{(1)}=\sum_m P_{2\omega,m}''=P_{2\omega,0}''/(1-r_{2\omega}^4).$$

First Backward Pass

It is necessary to consider two cases.

a. E_ω is perpendicular to the plane of incidence: There is no change, at $Z=L$, in the direction of the fundamental electric field and the nonlinear polarization produced by the backward wave has the same direction $\hat{p}$.

$$P_{2\omega,1}'=r_\omega^2P_{2\omega}'$$

and the power transmitted at $Z=L$ is

$$r_{2\omega}^2r_\omega^4P_{2\omega,0}''.$$

Taking into account the multiple reflections we get

$$P_{2\omega}''^{(2)}=[r_{2\omega}^2r_\omega^4/(1-r_{2\omega}^4)]P_{2\omega,0}''.$$

b. E_ω lies in the plane of incidence. There is a change in the direction of the electric field after reflection and the unit vector of the nonlinear polarization is $\hat{p}_R$ which corresponds to a projection factor $p_R(\theta)$. This projection factor can be calculated as we did for $p(\theta)$. $p_R(\theta)$ is generally close to $p(\theta)$. In some cases, a nonlinear coefficient other than d can be involved. In these conditions

$$P_{2\omega}''^{(2)}=[p_R^2(\theta)/p^2(\theta)][r_{2\omega}^2r_\omega^4/(1-r_{2\omega}^4)]P_{2\omega,0}''.$$

Second Forward Pass

During the second forward pass, the electric field of the fundamental wave is decreased by r_ω^2.

$$P_{2\omega}''^{(3)}=[r_\omega^8/(1-r_{2\omega}^4)]P_{2\omega,0}''$$

and so on. Summing all the contributions we see that the multiple reflections induce a correction factor $\mathfrak{R}(\theta)$

$$\mathfrak{R}(\theta)=[1/(1-r_{2\omega}^4)\,(1-r_\omega^8)]\times\{1+[p_R^2(\theta)/p^2(\theta)]r_{2\omega}^2r_\omega^4\}, \quad \text{(B6)}$$

where $p_R^2(\theta)=p^2(\theta)$ when the electric field at ω is perpendicular to the plane of incidence. At normal incidence $r=(n-1)/(n+1)$ and $r_{2\omega}$ has almost the same value as r_ω

$$\mathfrak{R}(0)=(1+r^6)/[(1-r^4)\,(1-r^8)]. \quad \text{(B7)}$$

It is obvious that $\mathfrak{R}(0)$ is close to unity for low values of the refractive index and therefore can be neglected. For $n=2$, $\mathfrak{R}(0)\simeq1.01$ while for $n=4$, $\mathfrak{R}(0)=1.20$ and the correction is no longer negligible.

It is worth noting that Eq. (B7) is identical with the case of a phase matching experiment, at normal incidence.[19]

APPENDIX C: BEAM SIZE CORRECTION

The previous calculations have been made assuming the electric field of the incident beam is of constant amplitude on the entire boundary surface $Z=0$. Hence we neglected the fact that the bound and free waves are not traveling in exactly the same direction inside the crystal.

This phenomenon reduces the interaction volume of the free and bound waves and, therefore, induces a correction, which we calculate for an incoming Gaussian beam.

Let x, y, z be a coordinate system such that

$$\hat{y}=\hat{Y}, \qquad \hat{z}=\mathbf{k}_\omega\,|\,k_\omega\,|^{-1}.$$

The electric field of the fundamental beam is[7]

$$E_\omega(x,y,z=\text{const})=E_\omega\exp\{-[(x^2+y^2)/w^2]\}\times\exp[-ik_\omega(x^2+y^2)/2R]. \quad \text{(C1)}$$

Experimentally the crystal is at the beam waist: w may be assumed to be independent of z, and R is infinite. In these conditions

$$E_\omega(X,Y,Z)=E_\omega\exp\left(-\frac{(X\cos\theta-Z\sin\theta)^2}{w^2}-\frac{Y^2}{w^2}\right). \quad \text{(C2)}$$

As a consequence of the boundary conditions we deduce

$$E_\omega'(X, Y, Z) = t_\omega' E_\omega \times \exp\left(-\frac{(X\cos\theta_\omega' - Z\sin\theta_\omega')^2\cos^2\theta}{w^2\cos^2\theta_\omega'} - \frac{Y^2}{w^2}\right). \quad \text{(C3)}$$

Let us consider now the wave equation for the second-harmonic inside the crystal

$$\nabla X \nabla \times \mathbf{E}_{2\omega}' + [\epsilon(2\omega)/c^2][\partial^2 \mathbf{E}_{2\omega}'/\partial t^2] = -(4\pi/c^2)(\partial^2 \mathcal{P}_{2\omega}'/\partial t^2). \quad \text{(C4)}$$

The transverse spatial variation of $\mathcal{P}_{2\omega}'$ is

$$\exp\left(-\frac{2(X\cos\theta_\omega' - Z\sin\theta_\omega')^2\cos^2\theta}{w^2\cos^2\theta_\omega'} - \frac{2Y^2}{w^2}\right). \quad \text{(C5)}$$

We do not solve Eq. (C4) exactly; we approximate the solution by assuming spatial variation factors for the amplitudes of the free and bound waves.

For the bound wave, this factor is given by (C5), and for the free wave it may be written as

$$\exp\left(-\frac{2(X\cos\theta_{2\omega}' - Z\sin\theta_{2\omega}')^2\cos^2\theta}{w^2\cos^2\theta_{2\omega}'} - \frac{2Y^2}{w^2}\right). \quad \text{(C6)}$$

In these conditions the solution of (C4) is

$$\mathbf{E}_{2\omega}' = \hat{e}_f E_f \exp\left(-\frac{2(X\cos\theta_{2\omega}' - Z\sin\theta_{2\omega}')^2\cos^2\theta}{w^2\cos^2\theta_{2\omega}'} - \frac{2Y^2}{w^2}\right)\exp(i\mathbf{k}_f\cdot\mathbf{r}) + \frac{4\pi\mathcal{P}_{2\omega}'}{n_\omega^2 - n_{2\omega}^2}\left(\hat{p} - \frac{\mathbf{k}_b(\mathbf{k}_b\cdot\hat{p})}{|k_f|^2}\right)\exp\left(-\frac{2(X\cos\theta_\omega' - Z\sin\theta_\omega')^2\cos^2\theta}{w^2\cos^2\theta_\omega'} - \frac{2Y^2}{w^2}\right)\exp(i\mathbf{k}_b\cdot\mathbf{r}).$$

Carrying out the calculations in the same manner as in Appendix A, we get for the intensity coming out of the crystal

$$I_{2\omega}'' = \frac{8\pi c\,|\mathcal{P}_{2\omega}'|^2}{(n_\omega^2 - n_{2\omega})^2} T_{2\omega}'' \exp\left(-\frac{4Y^2}{w^2}\right)\exp\left(-\frac{2(X\cos\theta_{2\omega}' - L\sin\theta_{2\omega}')^2\cos^2\theta}{w^2\cos^2\theta_\omega'} - \frac{2(X\cos\theta_\omega' - L\sin\theta_\omega')^2\cos^2\theta}{w^2\cos^2\theta_\omega'}\right)\sin^2\Psi.$$

The power $P_{2\omega}''$ is the flux of the intensity $I_{2\omega}''$ across the plane $Z = \text{const}$. Therefore,

$$P_{2\omega}'' = \int\int I_{2\omega}''\cos\theta\, dX\, dY.$$

Ψ is independent of X and Y.

Using

$$\int_{-\infty}^{\infty}\exp(-au^2)\,du = (\pi/a)^{1/2},$$

we get

$$P_{2\omega}'' = 2\pi^2 cw^2[|\mathcal{P}_{2\omega}'|^2/(n_\omega^2 - n_{2\omega}^2)^2]T_{2\omega}'' \times \exp[-(L^2/w^2)\cos^2\theta(tg\theta_\omega' - tg\theta_{2\omega}')^2]\sin^2\Psi. \quad \text{(C9)}$$

Equation (C9) shows that the correction factor taking into account the beam size effect is

$$\mathcal{B}(\theta) = \exp[-(L^2/w^2)\cos^2\theta(\tan\theta_\omega' - \tan\theta_{2\omega}')^2]. \quad \text{(C10)}$$

$\mathcal{B}(0) = \mathcal{B}(\pi/2) = 1$ but $\mathcal{B}$ may differ significantly from unity for θ in the range $(\pi/4, \pi/2)$ if $L \gg w$.

* On leave of absence from C.N.E.T., 92 ISSY les Mx, France.
† Currently at Philips Laboratories, Briarcliff Manor, New York.

[1] G. D. Boyd and D. A. Kleinman, J. Appl. Phys. **39,** 3597 (1968).
[2] G. E. Francois, Phys. Rev. **143,** 597 (1966).
[3] J. E. Bjorkholm and A. E. Siegman, Phys. Rev. **154,** 851 (1967).
[4] P. D. Maker, R. W. Terhune, M. Nisenoff, and C. M. Savage, Phys. Rev. Lett. **8,** 21 (1962).
[5] N. Bloembergen and P. S. Pershan, Phys. Rev. **128,** 606 (1962).
[6] J. Ducuing and N. Bloembergen, Phys. Rev. Lett. **10,** 474 (1963).
[7] R. C. Miller, D. A. Kleinman, and A. Savage, Phys. Rev. Lett. **11,** 146 (1963).
[8] J. P. van der Ziel and N. Bloembergen, Phys. Rev. **135,** A1662 (1964).
[9] V. S. Suvorov, A. S. Sonin, and I. S. Rez, Sov. Phys.—JETP **26,** 33 (1968).
[10] A. Savage, J. Appl. Phys. **36,** 1496 (1965).
[11] J. Jerphagnon, Ann. Telecommunications **23,** 203 (1968).
[12] R. Bechmann and S. K. Kurtz, *Numerical Data and Functional Relationships, Group III: Crystal and Solid State Physics*, K. H. Hellwege and A. M. Hellwege, Eds. (Springer-Verlag, Berlin, 1970), Vol. 2, p. 167.
[13] D. A. Kleinman, Phys. Rev. **125,** 1977 (1962).
[14] H. Kogelnik, Bell Syst. Tech. J. **44,** 455 (1965).
[15] N. Bloembergen, *Nonlinear Optics* (W. A. Benjamin, Inc., New York, 1965) Chap. 5, p. 131.
[16] S. K. Kurtz and T. T. Perry, J. Appl. Phys. **39,** 3798 (1968).
[17] S. Singh (private communication).
[18] F. Zernike, J. Opt. Soc. Amer. **54,** 1215 (1964); **55,** 210E (1965).
[19] S. H. Wemple and M. DiDomenico, Jr., J. Appl. Phys. **40,** 735 (1969).